



NBSIR 85-3111

Development of Power System Measurements -- Quarterly Report July 1, 1984 to September 30, 1984

R. E. Hebner, Editor

U.S. DEPARTMENT OF COMMERCE
National Bureau of Standards
Center for Electronics and Electrical Engineering
Electrosystems Division
Gaithersburg, MD 20899

November 1984

Issued March 1985

Prepared for:
Department of Energy
Division of Electric Energy Systems
100 Independence Avenue, SW
Washington, DC 20585

QC
100
U56
85-3111
1984

NBSIR 85-3111

**DEVELOPMENT OF POWER SYSTEM
MEASUREMENTS -- QUARTERLY REPORT
JULY 1, 1984 TO
SEPTEMBER 30, 1984**

R. E. Hebner, Editor

U.S. DEPARTMENT OF COMMERCE
National Bureau of Standards
Center for Electronics and Electrical Engineering
Electrosystems Division
Gaithersburg, MD 20899

November 1984

Issued March 1985

Prepared for:
Department of Energy
Division of Electric Energy Systems
1000 Independence Avenue, SW
Washington, DC 20585



U.S. DEPARTMENT OF COMMERCE, Malcolm Baldrige, *Secretary*
NATIONAL BUREAU OF STANDARDS, Ernest Ambler, *Director*

Foreword

This report summarizes the progress on four technical investigations during the fourth quarter of FY 84. Although reasonable efforts have been made to ensure the reliability of the data presented, it must be emphasized that this is an interim report so that further experimentation and analysis may be performed before the conclusions from any of these investigations are formally published. It is therefore possible that some of the observations presented in this report will be modified, expanded, or clarified by our subsequent research.

TABLE OF CONTENTS

	Page
Foreword.	iii
LIST OF FIGURES	v
LIST OF TABLES.	vii
Abstract.	1
1. INTRODUCTION.	1
2. ELECTRIC AND MAGNETIC FIELD MEASUREMENTS Subtasks No. 01 and 02.	1
3. TECHNICAL ASSISTANCE FOR FUTURE INSULATION SYSTEMS RESEARCH Subtask No. 03.	5
3.1 Oxyfluoride Production in SF ₆ /O ₂ Mixtures.	8
3.2 Oxyfluoride and Nitrogen Oxide Production in SF ₆ /N ₂ Mixtures.	13
4. INTERFACIAL PHENOMENA IN LIQUIDS Subtask No. 04.	21
4.1 Interfacial Breakdown Studies	23
4.2 Electro-Optical Electric-Field Measurements	26
5. NANOSECOND BREAKDOWN IN POWER SYSTEM DIELECTRICS Subtask No. 05.	26
6. REFERENCES.	31

LIST OF FIGURES

	Page
Figure 1. Schematic view of monopolar line and ion counter with inlet located in the ground plane.	3
Figure 2. Measured space charge density for different line operating conditions as a function of volumetric air flow M through the ion counter.	4
Figure 3. Estimates of duct losses based on eq (1) of the text. Data are the same as figure 2. The values of ρ_0 are based on measurements of J and E and an assumed ion mobility of $1.4 \times 10^{-4} \text{ m}^2/\text{Vs}$ (positive ions).	6
Figure 4. Comparisons of measured air speeds near the ion counter inlet (1 cm above the ground plane) and the speed of the ion due to the electric field at the surface of the ground plane. Volumetric flow rates (M) were as shown	7
Figure 5. Measured absolute SOF_4 concentrations versus net charge transported for 40 μA negative corona in SF_6/O_2 mixtures containing the indicated percent-by-volume concentrations of O_2 . The "pure" SF_6 contained trace levels of O_2 which could not be accurately determined.	9
Figure 6. Measured absolute SOF_2 concentrations versus net charge transported for 40 μA negative corona in SF_6/O_2 mixtures containing the indicated percent-by-volume concentrations of O_2 . The "pure" SF_6 contained trace levels of O_2 which could not be accurately determined.	10
Figure 7. Measured absolute SO_2F_2 concentrations versus net charge transported for 40 μA negative corona in SF_6/O_2 mixtures containing the indicated percent-by-volume concentrations of O_2 . The "pure" SF_6 contained trace levels of O_2 which could not be accurately determined.	11
Figure 8. Calculated production rate constants k for electron collision induced dissociation processes in SF_6/O_2 mixtures at $E/N = 1 \times 10^{-15} \text{ Vm}^2$ from Masek, et al. [6].	14
Figure 9. Measured absolute CO_2 concentrations versus net charge transported for 40 μA negative corona in SF_6/O_2 mixtures containing the indicated percent-by-volume concentrations of O_2 . The "pure" SF_6 contained trace levels of O_2 which could not be accurately determined	15

LIST OF FIGURES (continued)

Page

- Figure 10. Measured absolute SO_2F_4 concentrations versus net charge transported for 40 μA negative corona in SF_6/N_2 mixtures containing trace amounts of H_2O and O_2 and the indicated percent-by-volume concentrations of N_2 16
- Figure 11. Measured absolute SO_2F_2 concentrations versus net charge transported for 40 μA negative corona in SF_6/N_2 mixtures containing trace amounts of H_2O and O_2 and the indicated percent-by-volume concentrations of N_2 17
- Figure 12. Measured absolute SO_2F_2 concentrations versus net charge transported for 40 μA negative corona in SF_6/N_2 mixtures containing trace amounts of H_2O and O_2 and the indicated percent-by-volume concentrations of N_2 18
- Figure 13. Measured absolute NO and N_2O concentrations versus net charge transported for 40 μA negative corona in an $\text{SF}_6/30\%\text{N}_2$ mixture. The vertical arrows indicate times when the discharge was turned off for more than 12 hours 20
- Figure 14. Preliminary test data investigating data-taking methods. The first column (1) is the run number; the second column (2) shows when an interface was used (N = no interface present, Y = interface in place); the third column (3) is the number of breakdowns which were observed for the specified conditions or procedure; the fourth column (4) tells the status of the oil, normal oil from the barrel, or degassed; the fifth column (5) tells the procedure used in separating the electrode halves: S means the electrode halves were split for a short time, L means for a long time, NO means that the electrodes were not opened, T=0, 1, 2, 5 refers to the number of minutes waited before ramping up the voltage again after the previous breakdown experiment, N*S means that the electrode halves were split many times which produced many bubbles (BUBS), NI means a new interface was installed before each breakdown; and NNI means that a new interface was not installed; the sixth column (6) refers to the condition of the pump circulating the liquid through the cell, CONT means the pump ran continuously, OFF-RMP means the pump was turned off during the application of voltage, OFF-ALL means the pump was off during the entire experiment, and the number in parentheses refers to the speed of the pump; the last column (7) is the mean and standard deviation (in parentheses) of the breakdown voltage for that experiment. All these data were taken at room temperature and with 60-Hz ac voltage 24

LIST OF FIGURES (continued)

Page

Figure 15. Breakdown voltage as a function of temperature for ac and dc voltages, with and without paper interfaces bridging the gap. The first column (1) tells when an interface was present (Y = yes, N = no); the second column (2) shows the number of breakdowns produced under the present conditions; the third column (3) is the temperature; the fourth column (4) describes the type of voltage applied; the fifth column (5) describes the location of the breakdown (--- means no interface was present, ALL refers to the breakdown voltage with the interface present making no distinction whether or not the breakdown occurred at the interface, BAI, or not at the interface, NAI); the sixth column (6) shows the percentage of breakdowns which occurred at the interface when an interface was present; the next two columns (7) and (8) are the mean breakdown voltages with the standard deviations in parentheses, both the ac peak values and rms values are shown, the rms values are plotted with the dc values in the horizontal graph. 25

Figure 16. Pulse forming components to provide nanosecond rise time pulses: (a) actual circuit, (b) simplified pulse-shaping configuration, after the first gap has shorted, neglecting the cell 28

LIST OF TABLES

Table 1. Limiting constant production rates, R_c , and deviations from linearity ϵ 22

Table 2. Limit constant production rates, R_c , and deviation from linearity ϵ 22

Table 3. Pulse shapes based on RLC component values 29

DEVELOPMENT OF POWER SYSTEM MEASUREMENTS — QUARTERLY REPORT
July 1, 1984 to September 30, 1984

R. E. Hebner, Editor

This report documents the progress on four technical investigations sponsored by the Department of Energy and performed by or under a grant from the Electrosystems Division, the National Bureau of Standards. The work described covers the period from July 1, 1984 to September 30, 1984. The report emphasizes the errors associated with measurements of electric and magnetic fields, the properties of corona in compressed SF₆ gas, the measurement of interfacial phenomena in transformer oil, and the measurement of dielectric properties on nanosecond time scales.

Key words: electric fields; gaseous insulation; interfaces: liquid insulation; magnetic fields; partial discharges; SF₆; solid insulation; transformer oil.

1. INTRODUCTION

Under an interagency agreement between the U.S. Department of Energy and the National Bureau of Standards, the Electrosystems Division, NBS, has been providing technical support for DOE's research on electric energy systems. This support has been concentrated on the measurement of electric and magnetic fields, the measurement of interfacial phenomena and of partial discharge phenomena, and the measurement of dielectric properties on nanosecond time scales. The technical progress made during the quarter July 1, 1984 to September 30, 1984 is summarized in this report.

2. ELECTRIC FIELD MEASUREMENTS

Subtasks Nos. 01 and 02

The objectives of this investigation are to develop methods to evaluate and calibrate instruments which are used, or are being developed, to measure the electric field, the space charge density, and current density in the vicinity of high-voltage dc transmission lines and in apparatus designed to simulate the transmission line environment; to provide electrical measurement support for DOE-funded efforts to determine the effects of ac fields on biological systems, and to provide similar support for biological studies which will be funded by the State of New York.

During the present quarter, measurements of ion density were made with an aspirator type ion counter operating in the ground plane, in the presence of an external dc electric field. The influence of the external electric field on density measurements was examined by varying the field strength and air flow rate through the ion counter.

The operation of aspiration devices such as ion counters, conductivity tubes and filtration devices can be affected by the presence of large external fields such as those found near HVDC transmission lines or some biological exposure systems. Laboratory studies are being done at NBS to understand the

magnitude of errors introduced by these external fields and to determine optimum conditions for operating these instruments. In a study reported earlier [1], an ion counter was operated above the ground plane under a monopolar line which was in corona. The experiment was configured such that the air flow through the ion counter could be varied. This feature and the use of inlets of different sizes allowed a wide variation in the air speeds near the inlet to the counter. The ion counter and associated electronics were isolated from ground so that the potential of the assembly, relative to space potential, could be varied. Measurements were taken in which the dependence of the measured ion density on (1) ion counter potential and (2) air speed at the inlet were determined. It was found that the indicated ion density depended strongly on ion counter potential as the potential approached the average space potential, and that for a grounded counter, the ion density fell off as the air speed at the inlet decreased. This latter result is generally consistent with a picture in which the ions are lost to the inlet walls of the ion counter as a result of the electric field, the influence of which increases as the air speed decreases.

Although operation of an ion counter above the ground plane offers a number of advantages in an outdoor setting, the enhancement of the external field near the inlet tends to augment any loss mechanisms that may be operating. Electric field effects can be minimized by locating the ion counter such that its inlet is in the ground plane. An experimental configuration similar to that used in the work described above was set up in the laboratory and is illustrated in figure 1. The ground plane was a table covered with aluminum as shown. The electric field was measured using a field mill, and current sensing plates were located on either side of the opening to the ion counter. The duct to the ion counter was made of metallic tubing and had a length of 0.4 m.

Measurements were made for three line operating conditions such that the electric field at the surface of the ground plane was 14.8, 20.8, or 29.8 kV/m. For each of these conditions, the flow rate through the ion counter was varied and the space charge density ρ was determined using the relation $\rho = I/M$, where I is the current measured by the ion counter and the volumetric flow rate through the counter is M . At the same time the electric field E and vertical current density J were also measured. The space charge density can be determined from the relation $\rho_0 = J/kE$, where k is an average mobility for the ions making up the ion current. Calculations for ρ_0 were made for each of the three operating conditions studied. The results of these calculations and the measurements are shown in figure 2. These are for positive corona and similar results were seen for negative corona.

Because of the length of the duct and the large ion densities, estimates were made of the losses in the connecting the ion counter to the inlet in the ground plane. These losses were estimated using the theory outlined by Kaune et al. in [2]. In reference [2], an equation relating the spatial dependence of space charge density at locations away from the source is given and a number of applications cited. This equation was applied to the motion of ions in a duct

$$\rho/\rho_0 = [1 + \rho_0(ku/\ell\epsilon_0)]^{-1} \quad (1)$$

where ρ_0 is the initial space charge density, u is the average ion speed in the duct, ℓ is the length of the duct, ϵ_0 is the permittivity of space, and k is the average ion mobility. Using ρ_0 calculated from the measurements of E and J , estimates were made of the expected duct losses using average speeds in

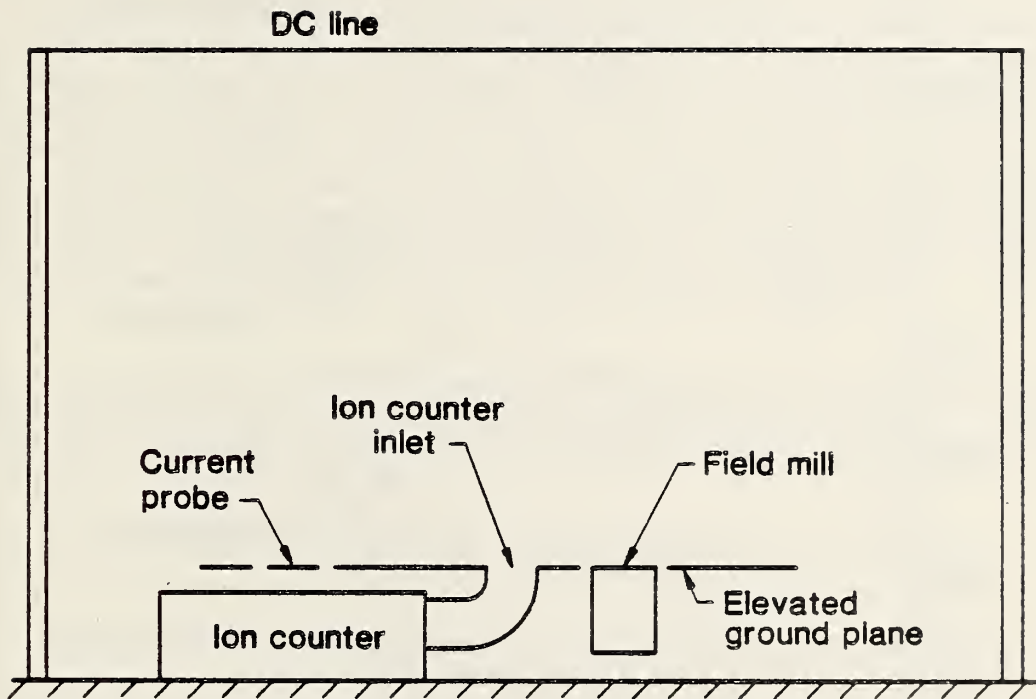


Figure 1. Schematic view of monopolar line and ion counter with inlet located in the ground plane.

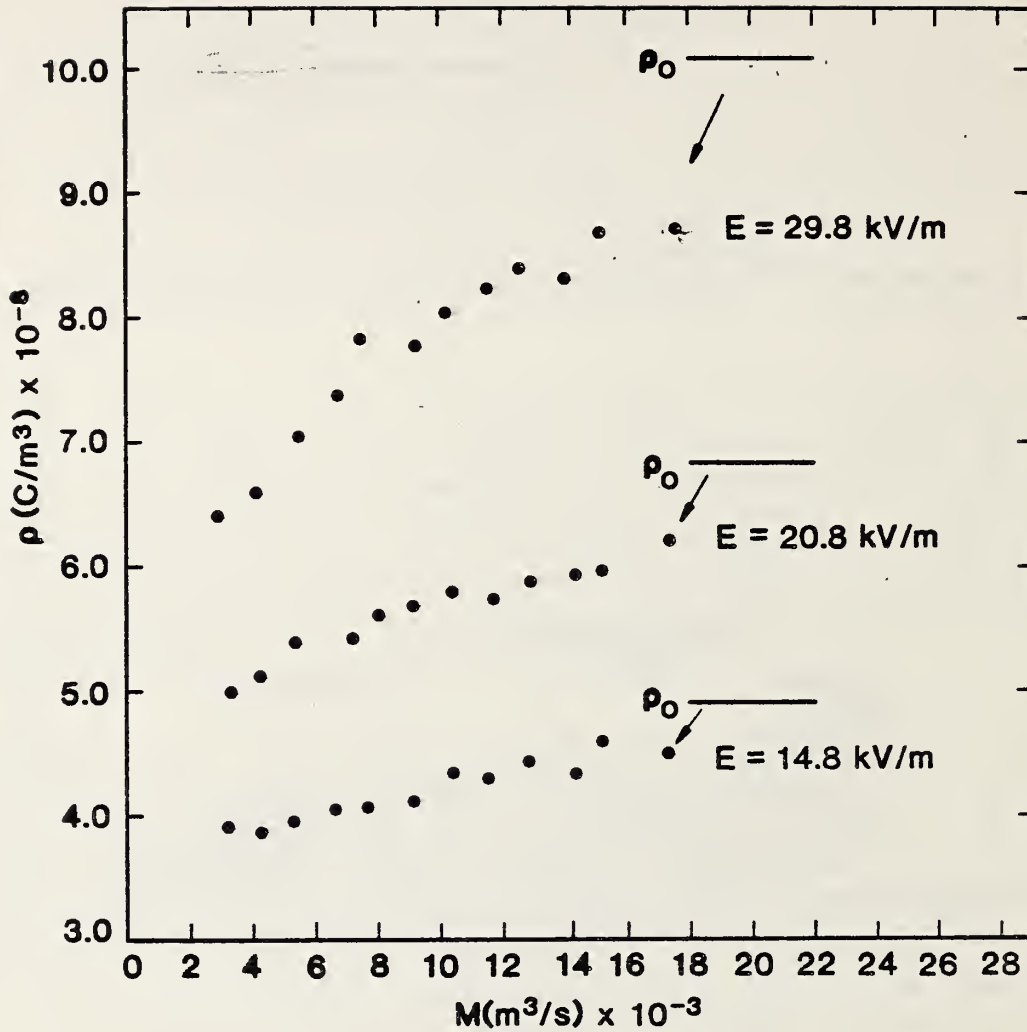


Figure 2. Measured space charge density for different line operating conditions as a function of volumetric air flow M through the ion counter.

the ducts, calculated by assuming uniform velocities and the measured volumetric air flow. The solid lines shown in figure 3 indicate the estimates of the space charge density transmitted through the duct, starting with the initial ion density ρ_0 . An additional set of measurements was made using a longer duct and similar results were observed. It is clear that most of the losses appear to be associated with duct losses. This is a puzzling result, since the electric fields near the inlet are such that ion motion should be dominated by the electric field forces. This is indicated in figure 4, which summarizes air speed measurements made 1 cm above the ion counter inlet using a hot film anemometer. Indicated for comparison are the drift speeds due to the ion moving in the electric field.

In order to gain a better understanding of the motion of ions in the electrohydrodynamic field near the inlet, modeling should be done. While the full three-dimensional solution to the problem appears prohibitive, simpler two dimensional models should yield significant information. Simpler modeling can be done by using finite element calculations of the electric field near the inlet and reasonable estimates of the air flow field. Additional experiments are also planned using the parallel plate system at NBS in which the electrical environment is better known than in the monopolar line configuration. Questions of the perturbation of the operation of the parallel plate system will have to be answered first and some effort in this area has been described previously [3].

During the next quarter, testing and calibration of a magnetic fieldmeter for measuring ambient ac magnetic fields will be completed. A space potential probe will be fabricated for measurements of potential in dc electric fields with space charge.

For further information contact Dr. M. Misakian at (301) 921-3121.

3. TECHNICAL ASSISTANCE FOR FUTURE INSULATION SYSTEMS RESEARCH Subtask No. 03

The objective of this project is to develop diagnostic techniques to monitor, identify, and predict degradation in future compressed gas electrical insulating systems under normal operating conditions. The focus is on the fundamental information and data needed to improve test design and performance evaluation criteria. The scope of the project encompasses the following investigations: 1) measurement and calculation of electric discharge inception in compressed electronegative gases; 2) measurement, calculation, and compilation of fundamental data on electron transport and electrical breakdown in gases; 3) measurement of absolute electric discharge-induced decomposition rates in gaseous dielectrics; and 4) examination of the influence of contaminants like water vapor on the performance of compressed gas-insulated systems. Emphasis is given in these investigations to the development and evaluation of new measurement techniques.

The planned activities for FY84 included:

- 1) Preparation of conference and archival papers presenting results of our measurements on the production rates for the oxyfluorides SOF_2 , SO_2F_2 and SOF_4 , and SO_2 and H_2O generated by corona discharges in SF_6 or $\text{SF}_6/\text{H}_2\text{O}$ mixtures;

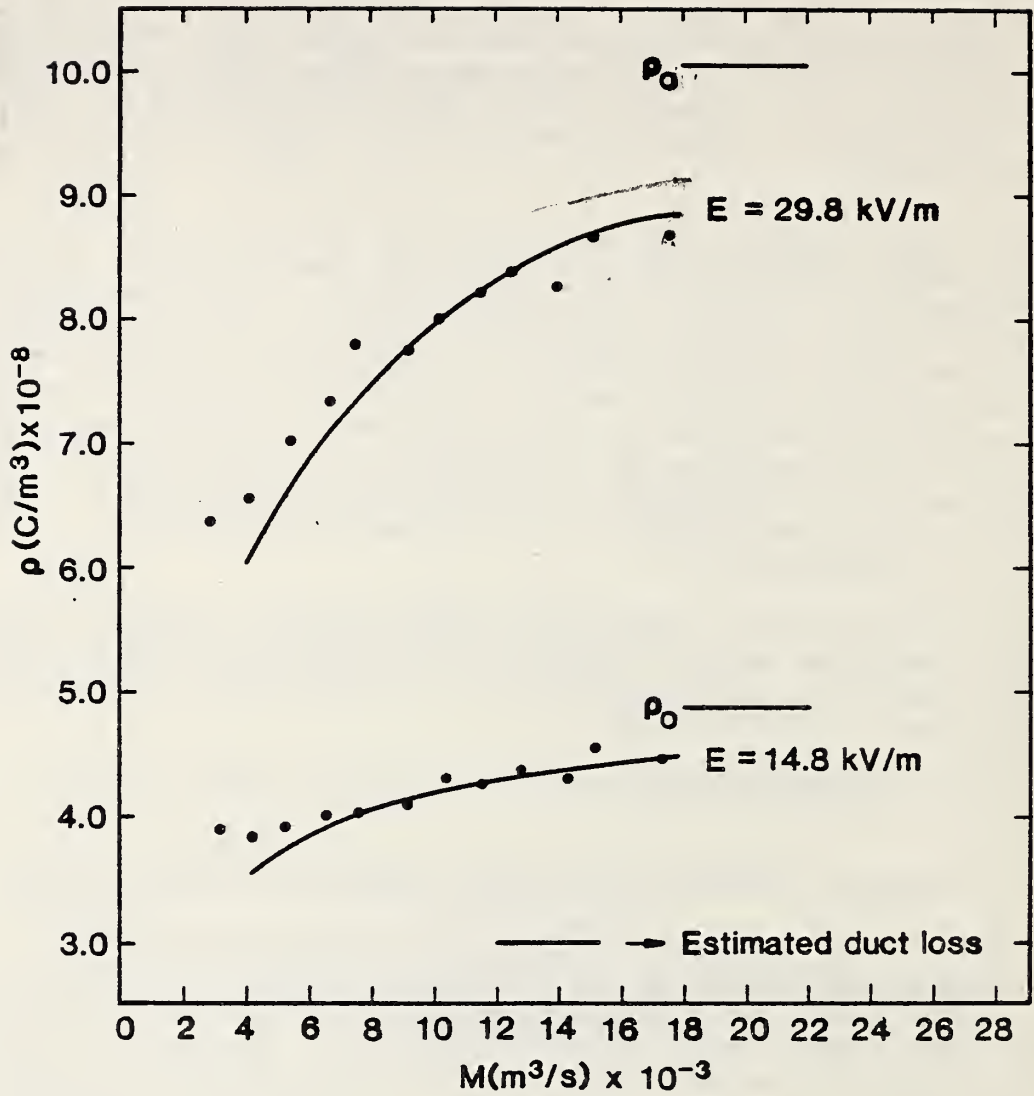


Figure 3. Estimates of duct losses based on eq (1) of the text. Data are the same as figure 2. The values of ρ_0 are based on measurements of J and E and an assumed ion mobility of $1.4 \times 10^{-4} \text{ m}^2/\text{Vs}$ (positive ions).

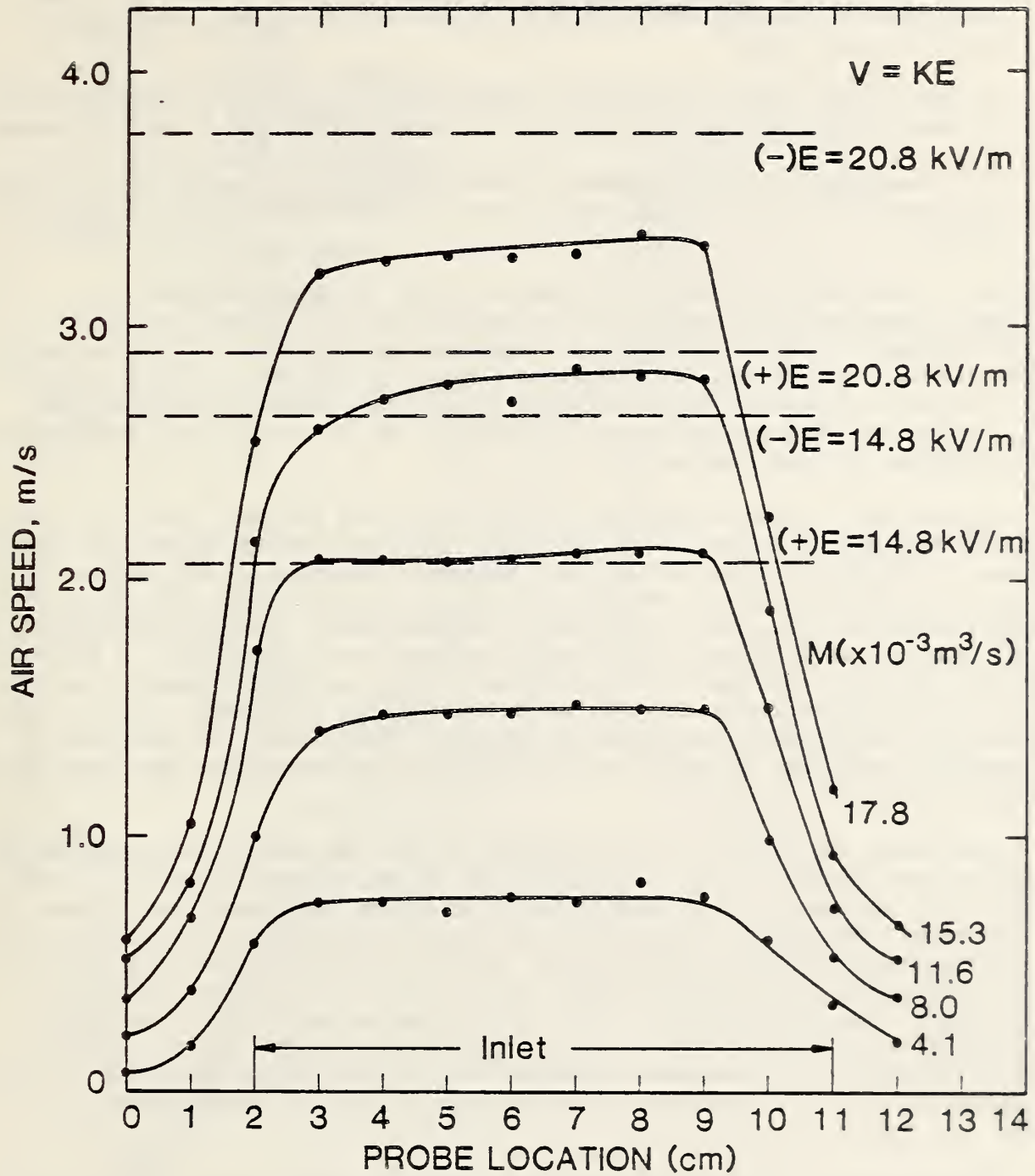


Figure 4. Comparisons of measured air speeds near the ion counter inlet (1 cm above the ground plane) and the speed of the ion due to the electric field at the surface of the ground plane. Volumetric flow rates (M) were as shown.

- 2) Extension of the measurements on by-product production rates in gas discharges to the mixtures, $\text{SF}_6 + \text{O}_2$, $\text{SF}_6 + \text{N}_2$, $\text{SF}_6 + \text{CO}_2$, and $\text{SF}_6 + \text{c-C}_4\text{F}_8 + \text{CHF}_3$;
- 3) Compilation of a computerized bibliography of electrical breakdown data in insulating gases and publication of this bibliography in an NBS report;
- 4) Investigation of the effects of trace quantities of water vapor on the enhancement of electron avalanche growth and corona discharge development in SF_6 .

Activity 1) has been completed. A paper entitled "Production Rates for discharge Generated SOF_2 , SO_2F_2 , and SO_2 in SF_6 and $\text{SF}_6/\text{H}_2\text{O}$ Mixtures" by R. J. Van Brunt, T. C. Lazo, and W. E. Anderson has appeared in the Proceedings of the Fourth International Symposium on Gaseous Dielectrics, Knoxville, 1984 [4], and an archival paper entitled "Production Rates for Oxyfluorides SOF_2 , SO_2F_2 , and SOF_4 in SF_6 Corona Discharges," by R. J. Van Brunt has recently been submitted for publication [5].

Considerable progress was made on activity 2) in the past year. It was decided, however, to focus on the first two mixtures, namely SF_6/N_2 and SF_6/O_2 , because of the significance of air as a common contaminant in SF_6 used as an insulant, and because of the possible importance of SF_6/N_2 and SF_6/air mixtures as substitutes for pure SF_6 in insulation applications. Preliminary results for SF_6/O_2 mixtures were presented in a previous quarterly report [6]. A paper discussing results obtained to date on both SF_6/O_2 and SF_6/N_2 mixtures has been submitted for presentation at the 37th Annual Gaseous Electronics Conference to be held in Boulder, Colorado, October 1984 [7]. The results of additional measurements performed on SF_6/O_2 and SF_6/N_2 mixtures during the past quarter are highlighted in this report.

Concerning activity 3), a bibliography of data on electrical breakdown in gases has been completed and is available as an NBS Technical Note [8]. The bibliography contains: 1) a list of archival papers and books that present data on electrical breakdown in gases and which have been published since 1950; 2) a computer generated index indicating the references that give particular types of data for each gas; 3) an author index; and 4) a list of relevant technical conferences. The bibliography, which is intended to serve as a guide in locating data on breakdown for a wide range of applications, can be obtained either from the U. S. Government Printing Office, Washington, DC 20402, or from the National Bureau of Standards, Electrosystems Division, Gaithersburg, MD 20899.

Although some progress was made on activity 4), this investigation remains incomplete. It is intended that the work on this activity will be completed in early FY 85.

3.1 Oxyfluoride Production in SF_6/O_2 Mixtures

Figures 5-7 show data for SOF_2 , SO_2F_2 , and SOF_4 production respectively in mixtures containing 1 to 10 percent O_2 in SF_6 compared with "pure" SF_6 containing only trace amounts of O_2 . Plotted are absolute concentrations in μmoles versus net charge transported in the discharge, i.e., discharge current \times time. The measurements for all these mixtures were performed at the same indicated total gas pressure and discharge current of 200 kPa and 40 μA

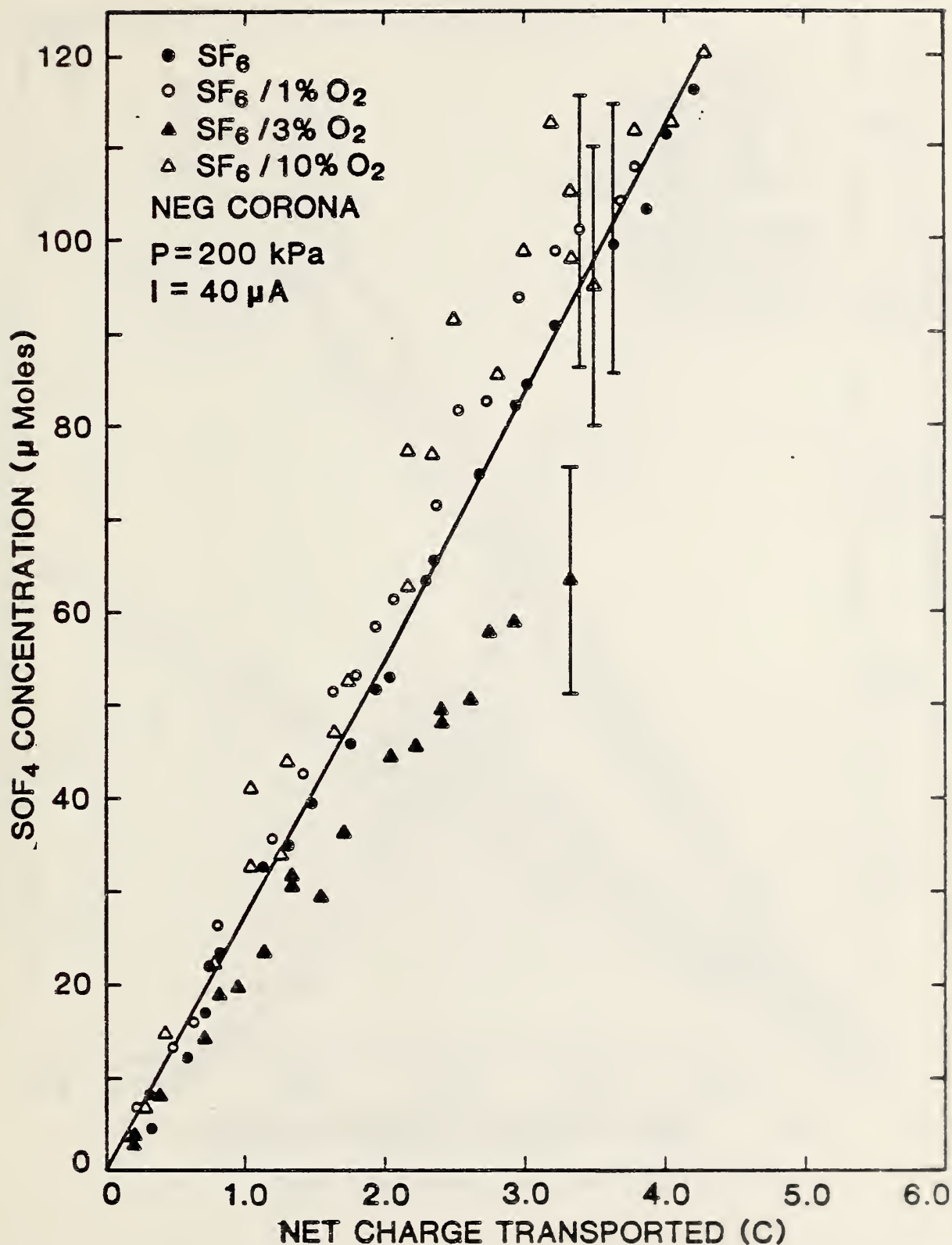


Figure 5. Measured absolute SOF₄ concentrations versus net charge transported for 40 μA negative corona in SF₆/O₂ mixtures containing the indicated percent-by-volume concentrations of O₂. The "pure" SF₆ contained trace levels of O₂ which could not be accurately determined.

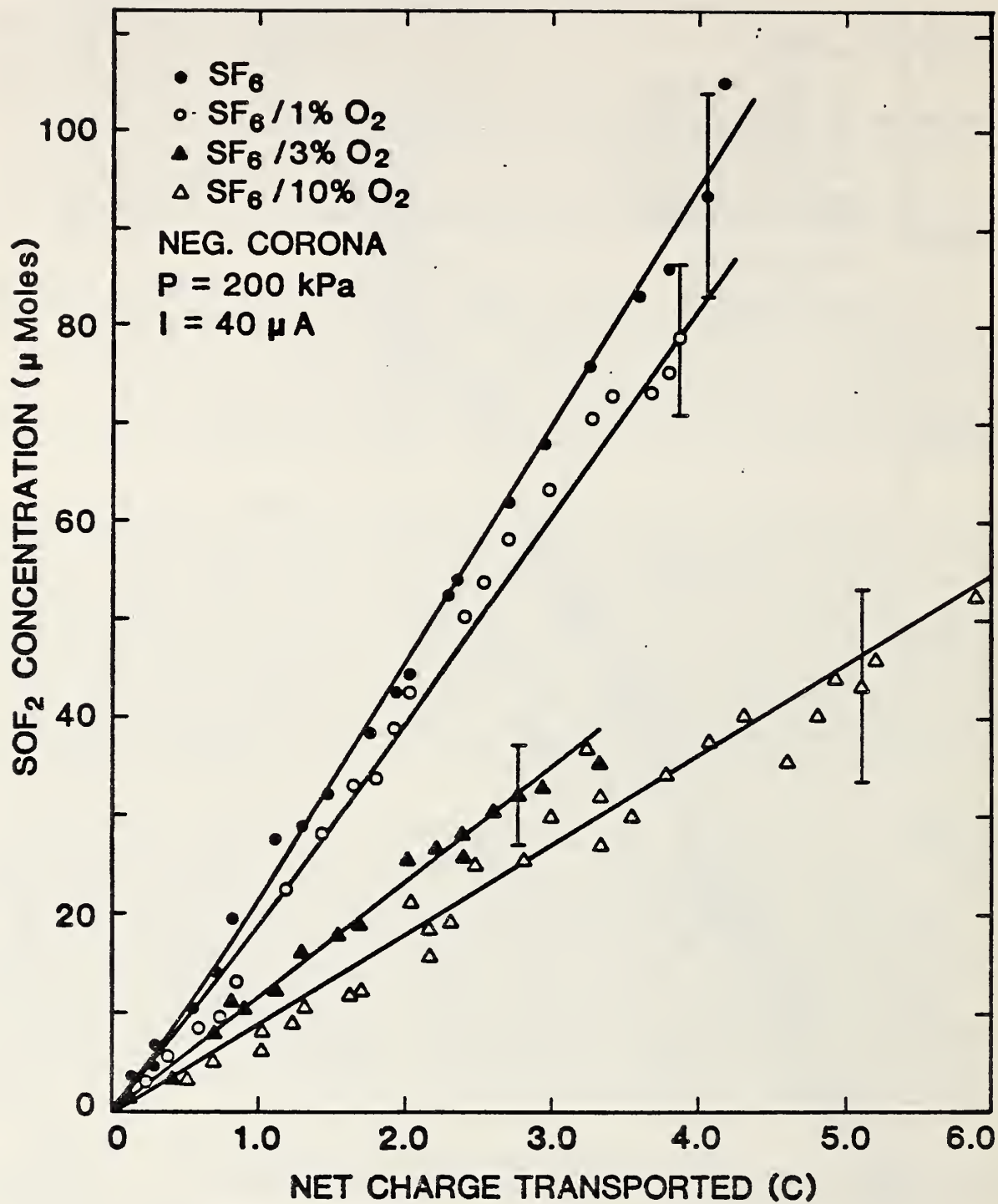


Figure 6. Measured absolute SOF₂ concentrations versus net charge transported for 40 μA negative corona in SF₆/O₂ mixtures containing the indicated percent-by-volume concentrations of O₂. The "pure" SF₆ contained trace levels of O₂ which could not be accurately determined.

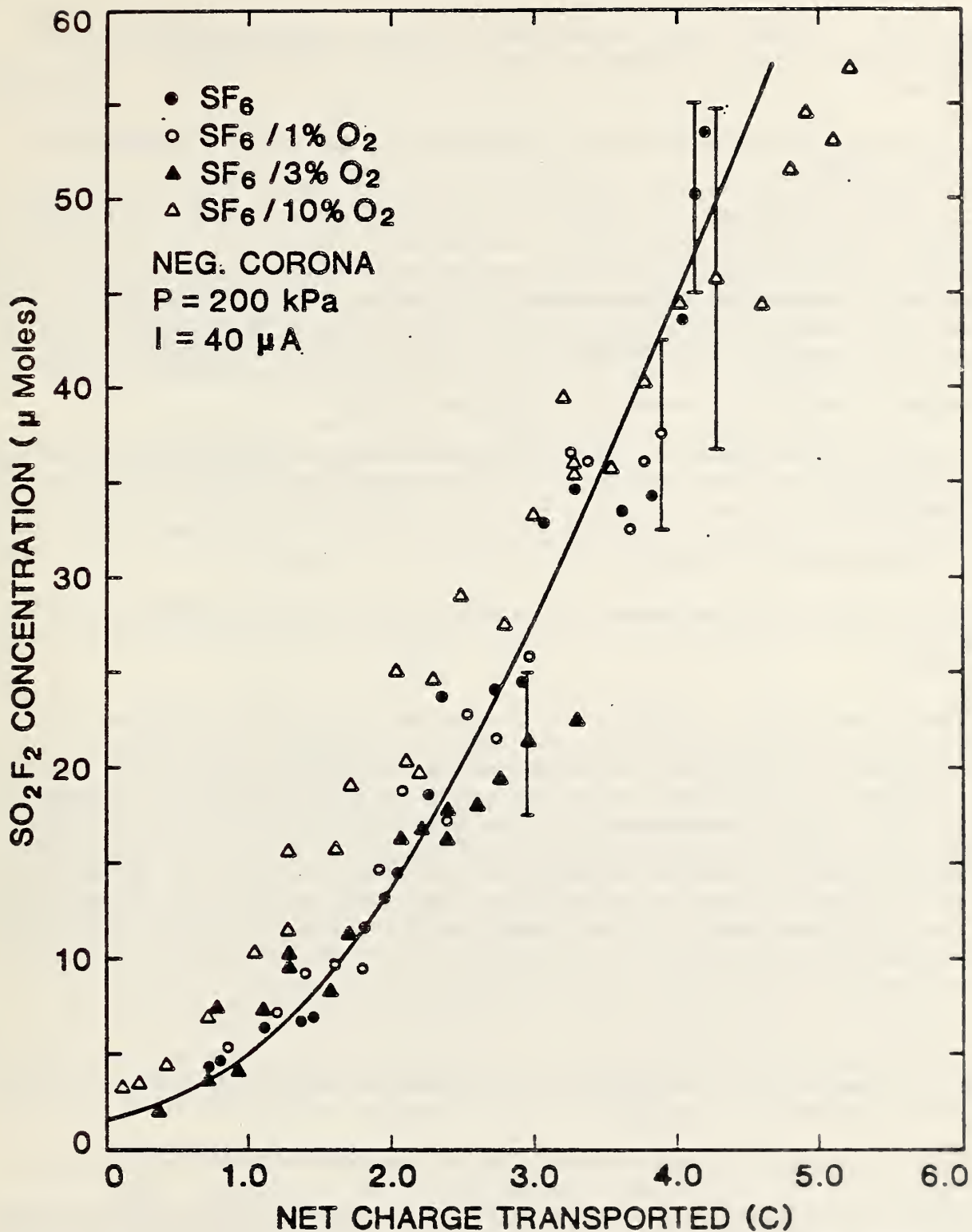


Figure 7. Measured absolute SO₂F₂ concentrations versus net charge transported for 40 μA negative corona in SF₆/O₂ mixtures containing the indicated percent-by-volume concentrations of O₂. The "pure" SF₆ contained trace levels of O₂ which could not be accurately determined.

respectively. In table 1 the corresponding limiting constant charge rates-of-production R_c are listed for the different SF_6/O_2 mixtures considered.

The charge rate-of-production R_c is related to the usual time rate-of-production dc/dt by

$$R_c = dc/dQ = (dc/dt)i^{-1}, \quad (2)$$

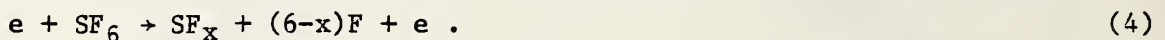
where i is the discharge current which was held constant in these experiments, Q is the charge transported by the current i , c is the concentration of the species under consideration, and t is time. The values of R_c in table 1 are obtained from the slopes of straight lines fit to the upper portions of the curves shown in figures 5-7 for $Q < Q_{min}$, where Q_{min} is the minimum value of the charge for which the assumption of linearity holds.

In general the production curves exhibit deviations from linearity that are most evident at the lowest values of Q , and are best described over the entire range by the form

$$c(Q) = c_0 + RQ^{1+\epsilon}, \quad (3)$$

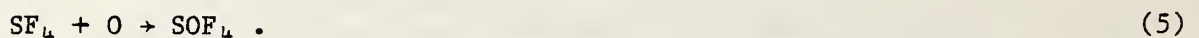
where c_0 , R , and ϵ are constants. The values of ϵ , which are a measure of deviations from linearity, are also given in table 1 for fits of the form given by eq (3).

The R_c results for the 3% O_2 mixture are more uncertain than those for the other mixtures because of the lower range of Q covered. Within the uncertainties indicated, the results demonstrate that the addition of 1 percent O_2 has virtually no influence on the production of the oxyfluorides. However, at higher O_2 content, changes occur in the relative production of SOF_2 , SO_2F_2 , and SOF_4 which show possible influence of gas-phase O_2 on not only the dominant gas-phase reactions leading to oxyfluoride production, but also on the electron energy distribution in the discharge [6] as will be discussed below. The fact that the oxyfluoride yields are not significantly influenced by the introduction of 1 percent O_2 indicates that the production rates are principally controlled by the dissociation rate of SF_6 in the discharge, i.e. by the process

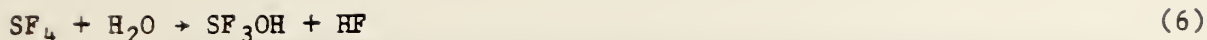


This is consistent with the suggested [5] mechanisms for SF_6 decomposition and oxyfluoride formation in corona.

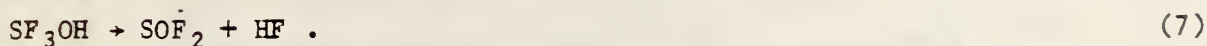
When O_2 is added at concentrations above 1 percent, the total oxyfluoride yield drops with the most dramatic effect on the SOF_2 production. The production of the other species drops slightly but does not significantly change for increases in O_2 concentration up to 10 percent. The drop in SOF_2 can be attributed to two possible effects: 1) a drop in the SF_6 dissociation rate when O_2 is added, and 2) a greater rate of SF_4 removal in the discharge due to the reaction



It will be recalled [4,5] that the most important mechanism for SOF_2 production is postulated to be hydrolysis of SF_4 in the bulk of the gas, i.e.,



followed by

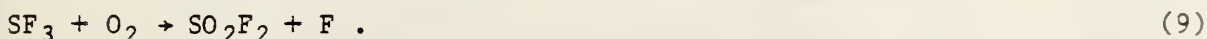


The effect of increasing the O_2 content in SF_6 on the electron energy distribution and thus on the dissociation rate of SF_6 in the gas has recently been considered in theoretical calculations of Masek, et al. [9] using numerical solutions of the Boltzmann Equation. Their calculations show that for a given electric field-to-gas density ratio (E/N), the mean electron energy in the gas shifts to lower energies as O_2 concentration increases. This gives rise to a lowering of the various ionization and dissociation rate constants with increasing O_2 content as shown in figure 8.

When O_2 is added, one can expect a higher relative concentration of O radicals in the discharge volume thereby enhancing the rate for reaction (5). However, the failure of the SOF_4 production to increase with increasing O_2 may again be indicative of a suppression in the SF_6 dissociation rate. The same consideration also applies to the interpretation of the SO_2F_2 data, since this species is expected to require O_2 for its formation through the reactions



and



The production of SOF_2 is likely to be more sensitive to changes in the discharge characteristics resulting from addition of O_2 , because its primary mechanism for production does not require the presence of this gas.

There is, of course, reason to doubt that the drop in SF_6 dissociation rate predicted by Masek, et al. is sufficient to entirely account for the observed decrease in SOF_2 production. Certainly some of this decrease could be due to a relative enhancement in the competitive removal of SF_4 by reaction (5). Measurements at higher O_2 concentrations are needed to help resolve this issue.

In addition to the oxyfluoride production rates, measurements were also made on CO_2 production in SF_6/O_2 mixtures as shown in figure 9. It is clear that CO_2 production goes up with increasing O_2 content, and shows some tendency to saturate at higher O_2 levels. Undoubtedly, production of this species is due to reactions of O_2 with carbon released from the stainless steel electrode.

3.2 Oxyfluoride and Nitrogen Oxide Production in SF_6/N_2 Mixtures

Measurements similar to those just described for SF_6/O_2 mixtures were also performed in SF_6/N_2 mixtures in which oxygen and water vapor were present at trace levels. Examples of results obtained for SOF_2 , SO_2F_2 , and SOF_4 production are shown in figures 10-12. Corresponding limiting constant charge rates-of-production are given in table 2. The most obvious effect of adding N_2 to SF_6 is a dramatic drop in the SOF_4 production. A statistically significant increase in SOF_2 production is also noted at the highest N_2 concentration. The production rate of SO_2F_2 appears to be relatively unaffected by N_2 content, at least for concentrations up 30 percent.

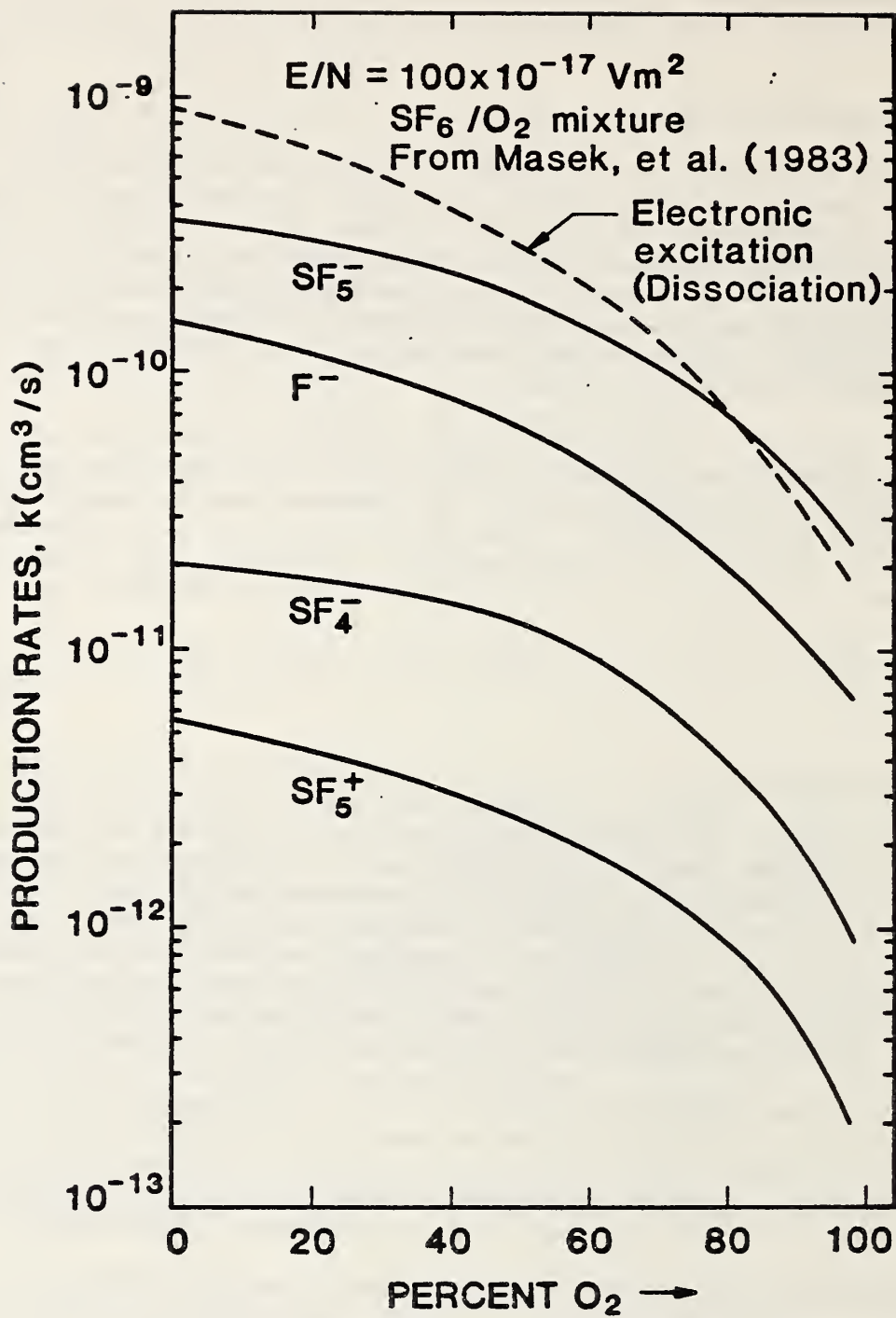


Figure 8. Calculated production rate constants k for electron collision induced dissociation processes in SF_6/O_2 mixtures at $E/N = 1 \times 10^{-15} \text{ Vm}^2$ from Masek, et al. [6].

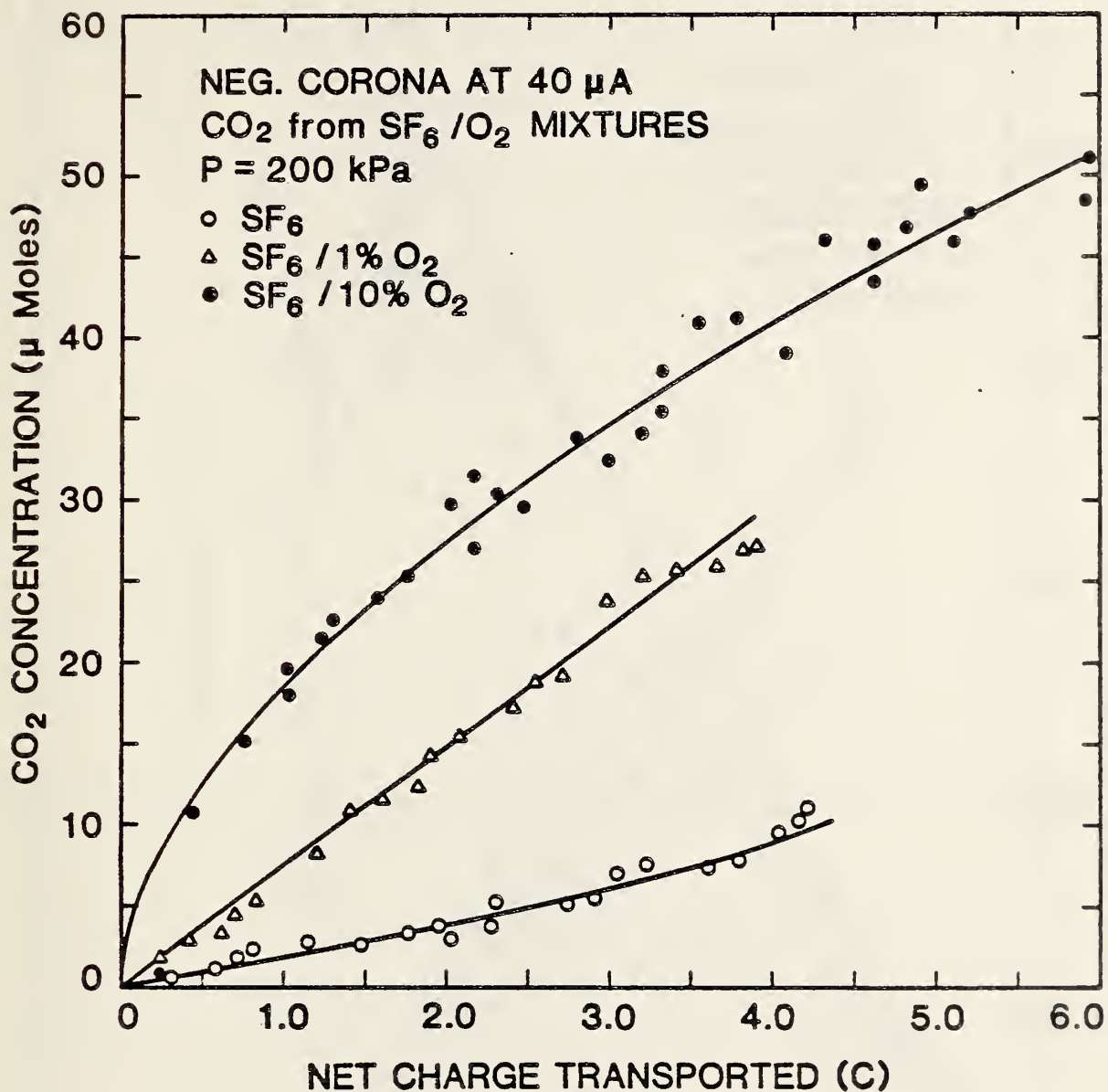


Figure 9. Measured absolute CO₂ concentrations versus net charge transported for 40 μ A negative corona in SF₆/O₂ mixtures containing the indicated percent-by-volume concentrations of O₂. The "pure" SF₆ contained trace levels of O₂ which could not be accurately determined.

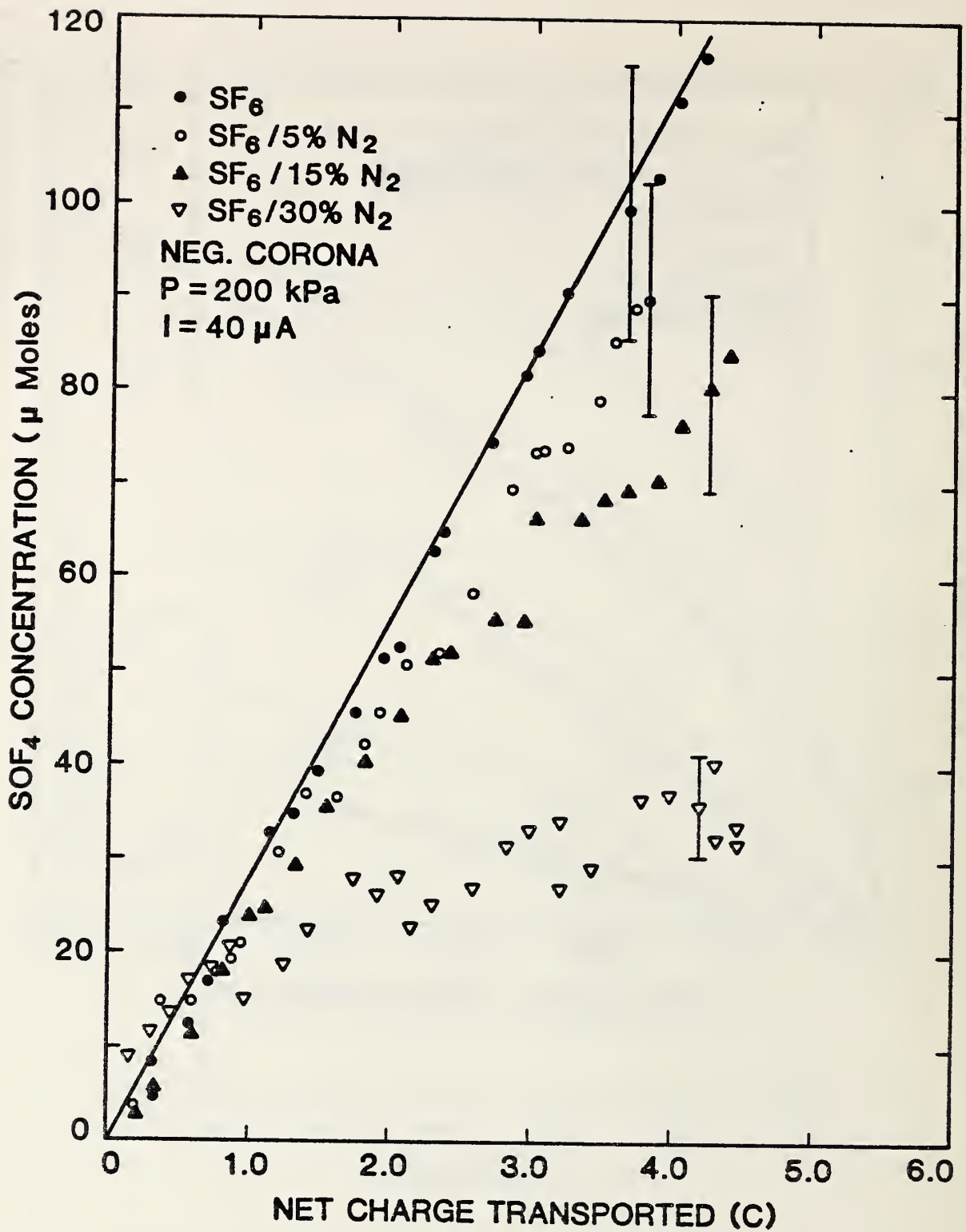


Figure 10. Measured absolute SOF₄ concentrations versus net charge transported for 40 μA negative corona in SF₆/N₂ mixtures containing trace amounts of H₂O and O₂ and the indicated percent-by-volume concentrations of N₂.

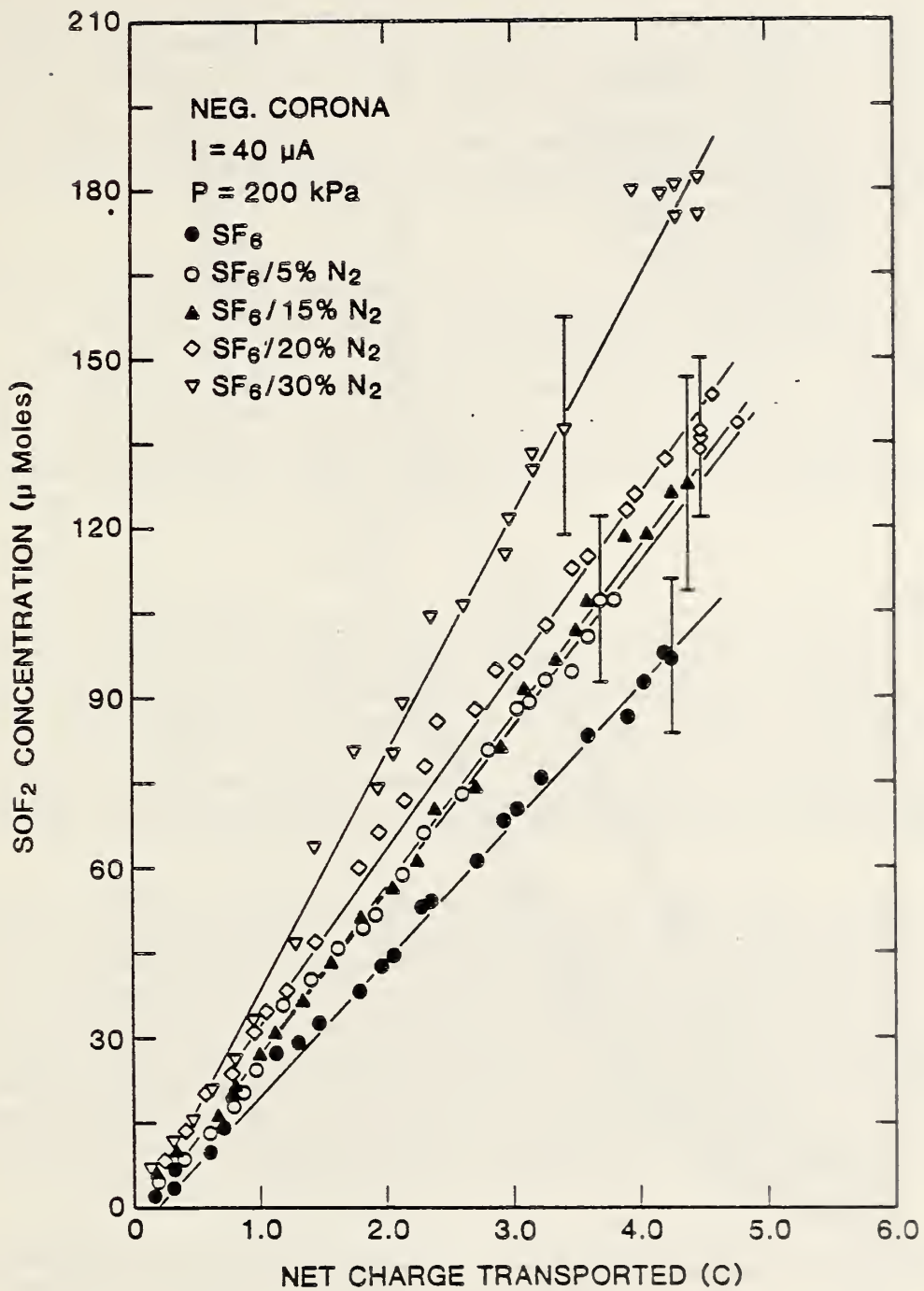


Figure 11. Measured absolute SOF_2 concentrations versus net charge transported for $40 \mu\text{A}$ negative corona in SF_6/N_2 mixtures containing trace amounts of H_2O and O_2 and the indicated percent-by-volume concentrations of N_2 .

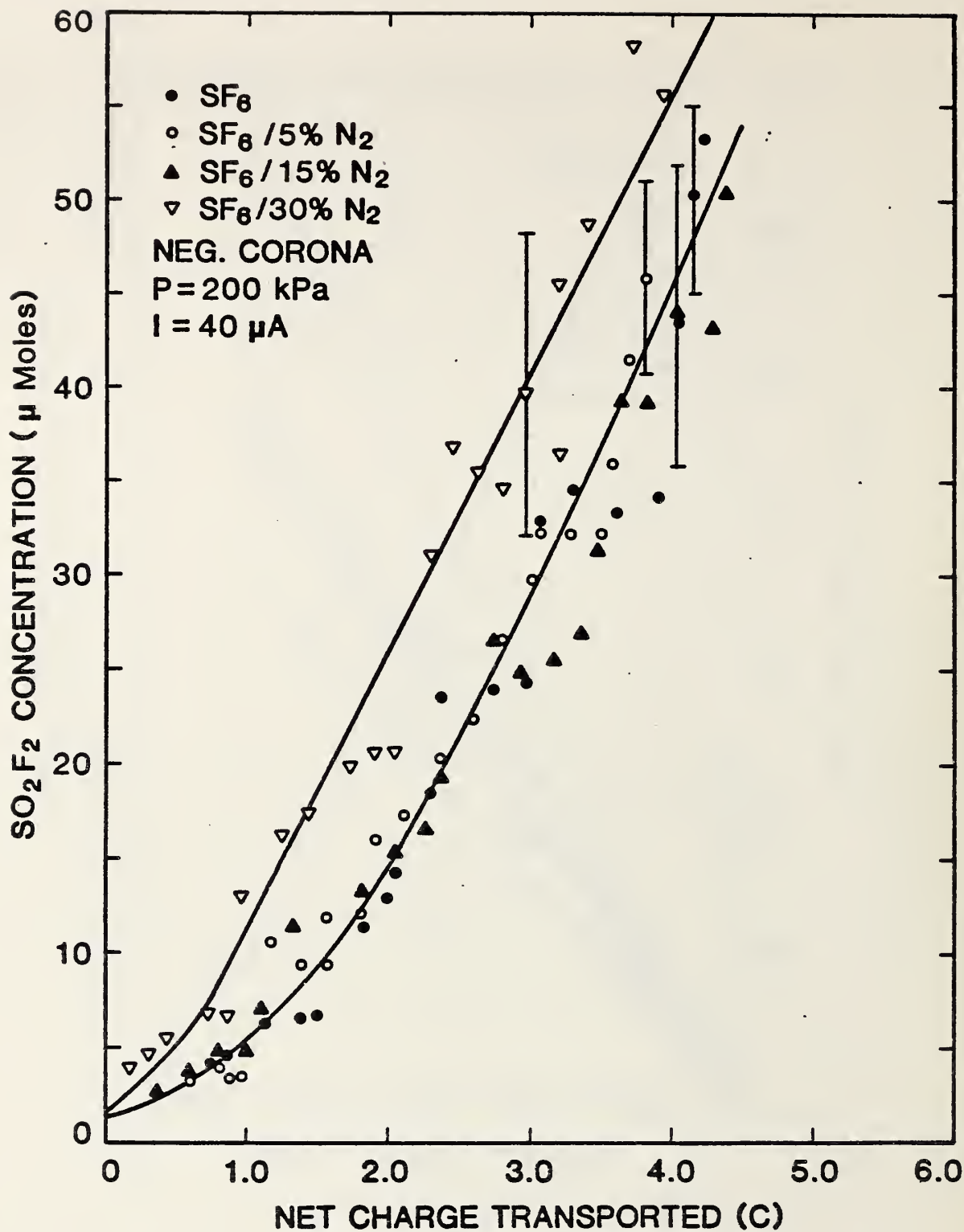


Figure 12. Measured absolute SO₂F₂ concentrations versus net charge transported for 40 μA negative corona in SF₆/N₂ mixtures containing trace amounts of H₂O and O₂ and the indicated percent-by-volume concentrations of N₂.

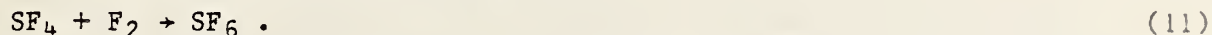
In the SF₆/30%N₂ mixture, production of the nitrogen oxides, especially NO, begins to become significant as seen in figure 13. For this mixture the NO yield is roughly comparable in magnitude to that for SOF₄, and the NO production curve showed only slight deviation from linearity. The production of NO₂ could not be observed by the method used. The yield for N₂O, as evident from figure 9, was observed to be an order of magnitude below that for NO. Moreover, the production curve for N₂O appeared to be highly nonlinear, suggesting that its production mechanism involves relatively weak secondary reactions in the gas phase.

At present one can only speculate about the processes that would be responsible for a selective decrease in the SOF₄ production relative to the production of the other oxyfluorides with increasing N₂ content. The effect is too large to be accounted for entirely by the decrease in relative SF₆ concentration. It is apparent that N₂ is effective in inhibiting those reactions that lead to SOF₄ formation. Since SOF₄ most likely requires the presence of O and OH free radicals in the discharge for its formation [5], reactions such as



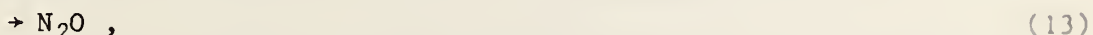
which can compete, for example, with reaction (5) in consuming oxygen containing free radicals could play a role in reducing SOF₄ production. However, reaction (10) is known to be quite slow [10], and the observed buildup of NO does not appear rapid enough to account for the decline in SOF₄ yield. Other mechanisms obviously deserve consideration in attempting to understand this effect. Of possible importance, for example, is the relative effectiveness of N₂ compared to SF₆ as a third body in stabilizing bimolecular formation of SOF₄ through processes like reaction (5).

A reduction in SOF₄ production, independent of the mechanism, should be accompanied by an increase in SOF₂ production as observed. This is expected on the basis of the expected predominant reactions involved in oxyfluoride formation [5]. If process (5) is inhibited for any reason, then more of the SF₄ produced by SF₆ dissociation and subsequent recombination processes can be expected to escape the active discharge volume and react with H₂O in the main bulk of the gas to give SOF₂ according to reactions (6) and (7). The increase in SOF₂ production, however, will necessarily be somewhat lower than the decrease in SOF₄ production because of the competitive influence of relatively fast recombination reactions such as [11]



This is also consistent with the present observations.

The failure of SO₂F₂ production to be significantly affected by N₂ at relative concentrations up to 30 percent is a reasonable expectation. The reactions



which could compete with reactions (8) and (9) in removing O₂ from the active discharge volume are expected on the basis of available reaction rate data [10]

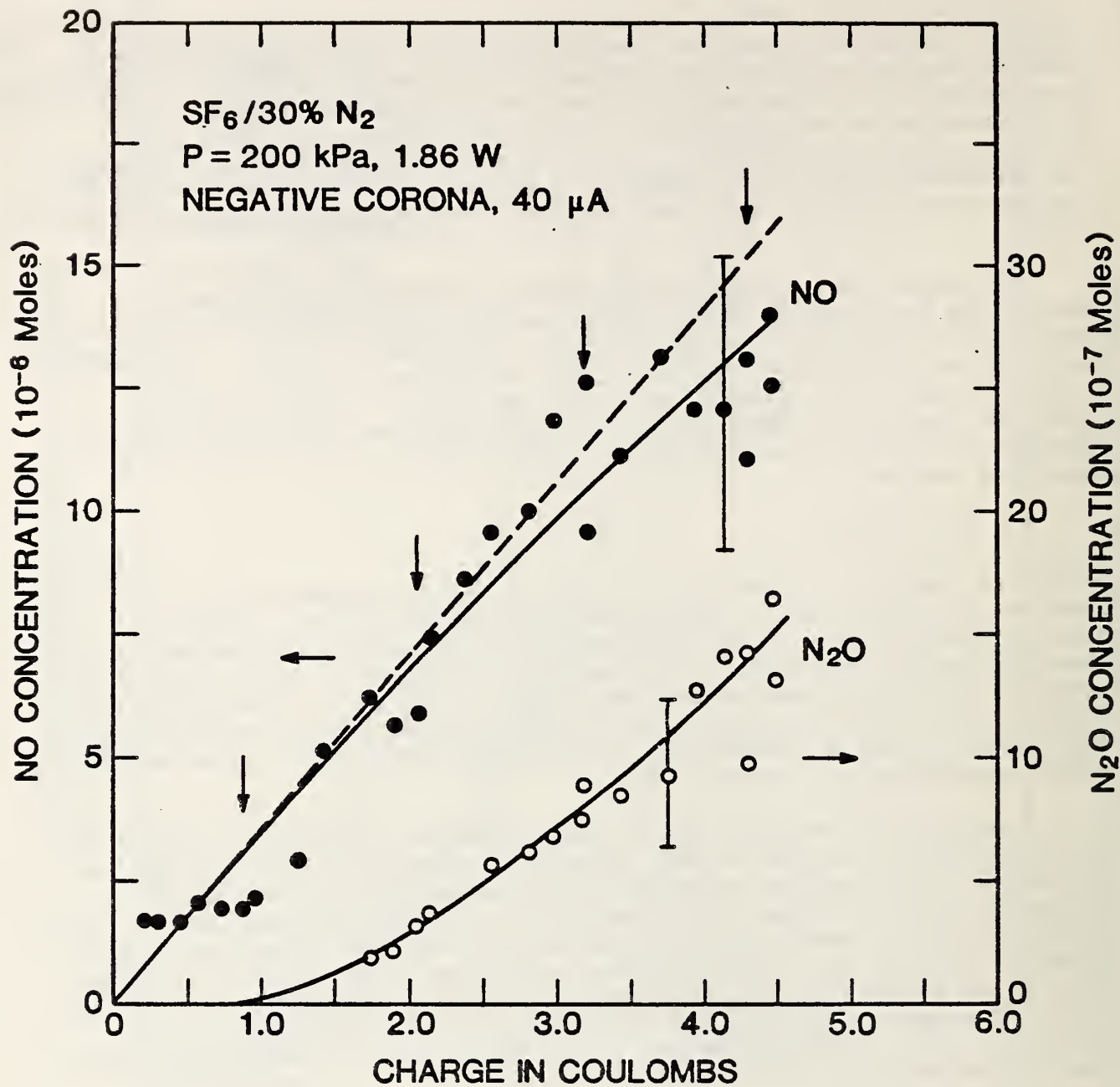


Figure 13. Measured absolute NO and N_2O concentrations versus net charge transported for $40 \mu A$ negative corona in an $SF_6/30\%N_2$ mixture. The vertical arrows indicate times when the discharge was turned off for more than 12 hours.

to be of minor importance. It is perhaps also worth noting that the production curves for SO_2F_2 appear to become more linear as N_2 content increases, i.e., $\epsilon \rightarrow 0$. On the other hand the corresponding SOF_4 production appears to become more nonlinear. This effect, if significant, could be indicative of the role played by the relatively slow reaction



which can occur in the bulk gas or on the walls of the discharge vessel [5]. At present, the uncertainties in the data are too great to enable one to draw firm conclusions about the relative importance of various reactions using observed deviations from linearity in the production curves.

During the next quarter, it is expected that more measurements will be made on oxyfluoride and nitrogen oxide production in SF_6/O_2 and SF_6/N_2 mixtures. Emphasis will be given to mixtures containing O_2 and N_2 concentrations which are higher than those considered in this report. Preliminary measurements may also be made on discharge by-product production rates using mixtures which contain isotopically pure $^{18}\text{O}_2$ and H_2^{18}O in order to determine that the mechanisms for oxyfluoride formation in SF_6 discharges are indeed those that have been postulated [2]. Further measurements will be performed to determine the influence of trace levels of water vapor on the statistical size distribution of electron avalanches in point-to-plane SF_6 discharges.

For further information contact Dr. R. J. Van Brunt at (301) 921-3121.

4. INTERFACIAL PHENOMENA IN LIQUIDS Subtask No. 04

The objective of this research is to develop techniques to measure the electrical behavior of liquid-solid composite insulation for use in high-voltage systems. Model systems of practical interest will be investigated, such as the interface between transformer oil and pressboard. The effects of contamination and temperature up to 150°C will be documented in these model systems in two ways: 1) breakdown measurements using high-speed photography, and 2) electro-optical measurements of the electric field in the vicinity of the interface. Such field measurements will provide understanding of the role of space charge and surface charge in high-voltage apparatus.

Up to this time, prebreakdown streamer propagation characteristics in many liquids and under a variety of circumstances have been documented and published. Additionally, streamer initiation studies have been started employing high optical magnification of the initiation point on the electrode. Studies into the effects of interfacial breakdown have revealed that the breakdown does not necessarily occur along a paper interface bridging the electrodes, nor is the interfacial breakdown voltage necessarily lower than in the liquid. An electro-optical, electric-field measurement system based on the Kerr effect has been successfully tested on transformer oil between parallel plates, with and without pressboard interfaces. With the oil used, significant space charge has been observed at elevated temperatures.

The research this quarter focused in two areas. First, interfacial breakdown probabilities were investigated using paper and oil which were not specially treated as in previous studies. Second, electro-optical field

Table 1. Limiting constant production rates, R_C , and deviations from linearity ϵ .

Gas Mixture	<u>SOF₄</u>		<u>SOF₂</u>		<u>SO₂F₂</u>	
	<u>R_C</u> (<u>μmoles/C</u>)	<u>ε</u>	<u>R_C</u> (<u>μmoles/C</u>)	<u>ε</u>	<u>R_C</u> (<u>μmoles/C</u>)	<u>ε</u>
SF ₆ /trace O ₂	30.2	0.077	24.7	0.077	15.9	0.805
SF ₆ /1%O ₂	29.8	-0.010	23.4	0.131	13.7	0.433
SF ₆ /3%O ₂	21.0	-0.055	14.8	0.011	6.6	0.000
SF ₆ /10%O ₂	23.4	-0.169	9.9	0.064	13.4	0.125

Table 2. Limit constant production rates, R_C , and deviation from linearity ϵ .

Gas Mixture	<u>SOF₄</u>		<u>SOF₂</u>		<u>SO₂F₂</u>	
	<u>R_C</u> (<u>μmoles/C</u>)	<u>ε</u>	<u>R_C</u> (<u>μmoles/C</u>)	<u>ε</u>	<u>R_C</u> (<u>μmoles/C</u>)	<u>ε</u>
SF ₆	30.2	0.077	24.7	0.077	15.9	0.805
SF ₆ /5%N ₂	20.5	0.037	30.4	0.077	15.7	0.840
SF ₆ /15%N ₂	18.4	-0.010	34.4	0.016	15.4	0.742
SF ₆ /30%N ₂	4.0	-0.580	45.6	0.075	14.7	0.024

measurements were made in the gap between a quasi-hyperbola electrode and a plane electrode. This latter work was performed in conjunction with a guest graduate student, Satish M. Mahajan, from the University of South Carolina. Both of these activities are summarized in this report.

4.1 Interfacial Breakdown Studies

In the quarterly report for the first quarter 1984, a cell design is presented which provides for changing a paper interface inside the cell without opening the cell [12]. A parallel-plate electrode geometry is provided by two cylinders with their ends facing each other. The edges of the cylinders are rounded so that the breakdowns occur randomly over the flat portion of the electrode faces. The cylinders are split in half along their axes. The halves of each cylinder can be separated so that a paper interface can be installed. When the cylinder halves are clamped together again one is left with a parallel-plate electrode system with paper bridging the gap between the electrodes. The outer diameter of the cylinders is 2.54 cm with the flat, parallel-plate region having a diameter of about 1.9cm. The gap between the electrodes is 0.246 cm.

In previous interfacial studies performed at NBS, much attention had been paid to the treatment of the oil and paper. The oxygen and water in the oil was removed by bubbling nitrogen through the oil for 48 hours or more, and then the oil was completely degassed under vacuum. The paper was vacuum baked at 125°C for at least 24 hours and then covered with the degassed oil, all under vacuum. Anticipating that water in the paper could be a source of stimulation for interfacial breakdown, no attempt was made to remove the water from the paper in the present experiment. The oil was degassed somewhat to increase its ability to dissolve post-breakdown bubbles to facilitate the taking of data.

To check the methods used to obtain the data, a series of trial experiments was made using different procedures to take the data. The results are shown in figure 14. The important lesson learned from this collection of data is that care must be exercised or the experiment will be biased by the experimental method used. One significant cause of the variation is that separating the electrodes generates bubbles in the transformer oil. If the voltage is turned on too soon, the bubbles in the split do not have sufficient time to dissolve in the oil and they cause breakdown. To minimize the effect of this potential problem yet keep the time to take the data down to a tolerable length, a one-minute interval was used as a minimum between each ramping of the voltage and any change which was made in the cell. Another important feature to note is that although the speed of the pump was not a factor, it was necessary that the pump remain on during the course of an experiment, apparently to remove or dilute the post-breakdown by-products.

The data on the probability of breakdown at the interface as a function of temperature are shown in figure 15. Both 60-Hz ac and dc were applied. The rms ac voltage is shown in figure 15. After each breakdown with an interface present a new interface was installed. Four temperatures were selected for study, but only when the temperature reached 150°C was there observed any obvious decrease in breakdown voltage. However, throughout these experiments when an interface was present the breakdown did not necessarily occur at the interface, and when the breakdown occurred at the interface the voltage was not

EXPERIMENTAL CONDITIONS

RN	I	#P	OIL	PROC	PUMP	VB (SD)
PA	N	10	NOM	SLS	CONT	75(16)
PB	N	10	NOM	SSSLSSS	CONT	84(11)
PC	N	10	NOM	SSSLSSS	OFF-RMP	76(15)
PD	N	10	DEG	SSSLSSS	OFF-RMP	77 (4)
PE	N	10	DEG	NO T=1	CONT	95 (6)
PF	N	10	DEG	NO T=1	OFF-ALL	79 (6)
PG	N	10	DEG	NO T=0	OFF-ALL	80 (6)
PH	N	10	DEG	SSS T=0	OFF-ALL	74 (5)
PI	N	5	DEG	N*S BUBS	OFF-ALL	71 (5)
PJ	N	10	DEG	NO T=0	CONT	83 (7)
PK	N	10	DEG	NO T=1	CONT	95 (5)
PL	N	5	DEG	NO T=0	CONT	88(15)
PL	N	5	DEG	NO T=1	CONT	98(13)
PL	N	5	DEG	NO T=2	CONT	96(12)
PL	N	5	DEG	NO T=5	CONT	100(11)
PM	N	7	DEG	NO T=1	CONT(6)	96 (9)
PM	N	7	DEG	NO T=1	CONT(2)	99 (6)
PM	N	7	DEG	NO T=1	CONT(8)	96(10)
PN	Y	5	DEG	NNI T=1	CONT(5)	98 (9)
PN	Y	5	DEG	NNI:5*S T=1	CONT(5)	99 (3)
PN	Y	5	DEG	NI T=1	CONT(5)	94 (7)

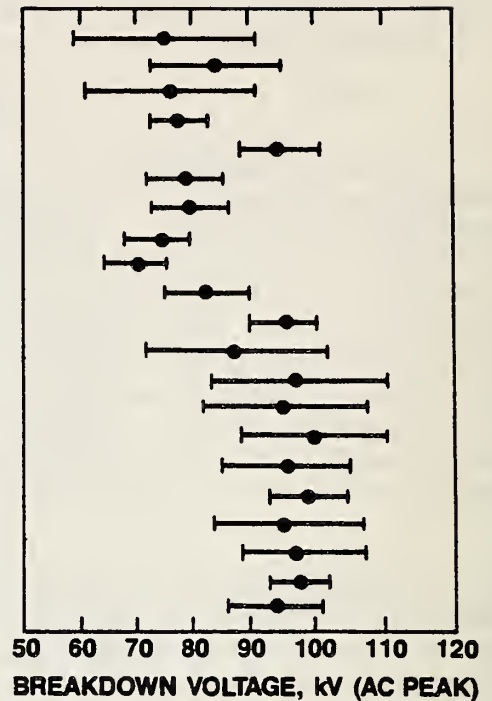


Figure 14. Preliminary test data investigating data-taking methods. The first column (1) is the run number; the second column (2) shows when an interface was used (N = no interface present, Y = interface in place); the third column (3) is the number of breakdowns which were observed for the specified conditions or procedure; the fourth column (4) tells the status of the oil, normal oil from the barrel, or degassed; the fifth column (5) tells the procedure used in separating the electrode halves: S means the electrode halves were split for a short time, L means for a long time, NO means that the electrodes were not opened, T=0, 1, 2, 5 refers to the number of minutes waited before ramping up the voltage again after the previous breakdown experiment, N*S means that the electrode halves were split many times which produced many bubbles (BUBS), NI means a new interface was installed before each breakdown; and NNI means that a new interface was not installed; the sixth column (6) refers to the condition of the pump circulating the liquid through the cell, CONT means the pump ran continuously, OFF-RMP means the pump was turned off during the application of voltage, OFF-ALL means the pump was off during the entire experiment, and the number in parentheses refers to the speed of the pump; the last column (7) is the mean and standard deviation (in parentheses) of the breakdown voltage for that experiment. All these data were taken at room temperature and with 60-Hz ac voltage.

EXPERIMENTAL CONDITIONS

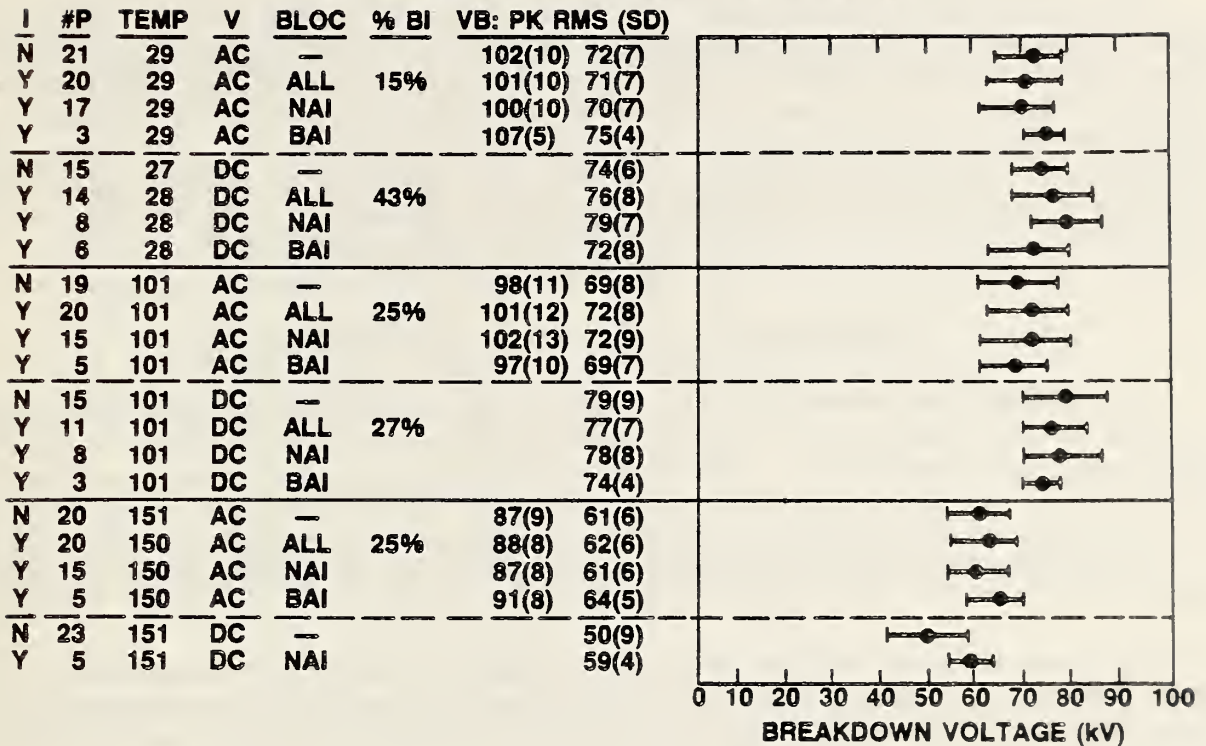


Figure 15. Breakdown voltage as a function of temperature for ac and dc voltages, with and without paper interfaces bridging the gap. The first column (1) tells when an interface was present (Y = yes, N = no); the second column (2) shows the number of breakdowns produced under the present conditions; the third column (3) is the temperature; the fourth column (4) describes the type of voltage applied; the fifth column (5) describes the location of the breakdown (--- means no interface was present, ALL refers to the breakdown voltage with the interface present making no distinction whether or not the breakdown occurred at the interface, BAI, or not at the interface, NAI); the sixth column (6) shows the percentage of breakdowns which occurred at the interface when an interface was present; the next two columns (7) and (8) are the mean breakdown voltages with the standard deviations in parentheses, both the ac peak values and rms values are shown, the rms values are plotted with the dc values in the horizontal graph.

necessarily lower than when the breakdown did not occur at the interface. These data confirm earlier results for this type of experiment.

It is important to note that at 100°C it was necessary to wait until the paper on the spools stopped releasing bubbles which were assumed to be water vapor coming from the water in the unprepared paper. It is not practical to take data while the bubbling continues because the application of voltage quickly brings all nearby bubbles into the region between the electrodes. The phenomenon of bubbles coming from the paper begins again at around 185°C. Under the assumption that some component of the paper material is vaporizing, no data were taken. Thus, with the paper used, data were taken only up to 150°C. However, the cell system endured higher temperatures successfully.

4.2 Electro-Optical Electric-Field Measurements

The second area researched this quarter is the electro-optical measurement of field between the tip of a hyperbola-like electrode over a plane -- a two dimensional field geometry. This work was performed in conjunction with Satish M. Mahajan of the University of South Carolina. These data are being analyzed. It is anticipated that the results of a comparison of a computer prediction of the field with the electro-optical measurements will be available in the near future.

An archival paper will be produced documenting the field enhancement due to space charge in various transformer oils between parallel-plate electrodes. The study will provide information for a range of temperatures and electrode materials.

An archival paper will be written documenting the results obtained above concerning the breakdown probability near a paper interface bridging the electrodes, as a function of temperature.

For further information contact Dr. E. F. Kelley at (301) 921-3121.

5. NANOSECOND BREAKDOWN IN POWER SYSTEM DIELECTRICS Subtask No. 05

The objectives of this effort are to develop measurement capabilities and provide data in support of the DOE program concerned with the effects of fast-rising electrical signals on electric power systems. Whereas the effects of microsecond rise-time pulses are reasonably well understood, the effects of nanosecond rise-time pulses on power system dielectrics are not well known. Appropriate model test systems will be developed along with the necessary measurement techniques.

The first step in understanding nanosecond breakdown in power system apparatus is to develop model systems to investigate nanosecond breakdown. To do this, it is necessary to design a circuit which will provide selectable rise times and fall times at voltages sufficiently high to cause streamer initiation. Additionally, measurement systems must also be developed to monitor the voltage waveform present at the electrodes. To meet these objectives, the following research has been accomplished:

1. Nanosecond Divider Tests: A 10 k Ω noninductive resistor divider was designed having a low-side resistance of 50 Ω . Using step response testing methods, it was shown to have a rise time of 3 ns or faster. Such speeds are sufficient to monitor the initial experiments which will be concerned with minimum voltage rise times of 5 ns. The divider is small enough to fit inside a breakdown cell and attach to the electrode to which voltage is applied.
2. Modeling of the Proposed Test Circuit: Figure 16 shows the proposed test circuit which will permit the selection of the rise time and fall time of the pulses applied to the test cell. The analysis of this simple system is straight forward using the equivalent circuit shown in figure 16b. The first gap in figure 16a is represented by a switch. The gap in the test cell is not shown for purposes of calculation, but, if present, it would appear as a switch shorting the resistor. Assuming an increasing current I in the counter-clockwise direction, the total voltage must sum to zero:

$$LdI/dt + RI + Q/C = 0. \quad (15)$$

Here Q is the charge on the capacitor. The solution to the homogeneous equation is a linear superposition of two exponentials which is written:

$$Q = Ae^{-at} + Be^{-bt} \quad (16)$$

where

$$\begin{aligned} a &= (R/2L)[1 + \sqrt{(1 - 4L/R^2C)^{1/2}}], \\ b &= (R/2L)[1 - \sqrt{(1 - 4L/R^2C)^{1/2}}]. \end{aligned} \quad (17)$$

Examining this solution, it is clear that oscillations are avoided if $4L/R^2C < 1$, which turns out not to be too restrictive.

To obtain the constants A and B, one invokes the initial conditions on $Q(t)$: $Q(0) = -CV_0$, and $dQ(0)/dt = 0$. From these initial conditions the constants are found to be

$$A = bCV_0/(a-b), \quad B = -aCV_0/(a-b). \quad (18)$$

The voltage across the load resistor R will then be given by $V = RdQ/dt$. For analysis, it is convenient to normalize to the applied voltage;

$$U = V/V_0 = (1-4L/R^2C)^{-1/2} [e^{-bt} - e^{-at}]. \quad (19)$$

If we assume that

$$4L/R^2C \ll 1, \quad (20)$$

then the constants simplify to

$$a = R/L, \text{ and } b = 1/RC; \quad (21)$$

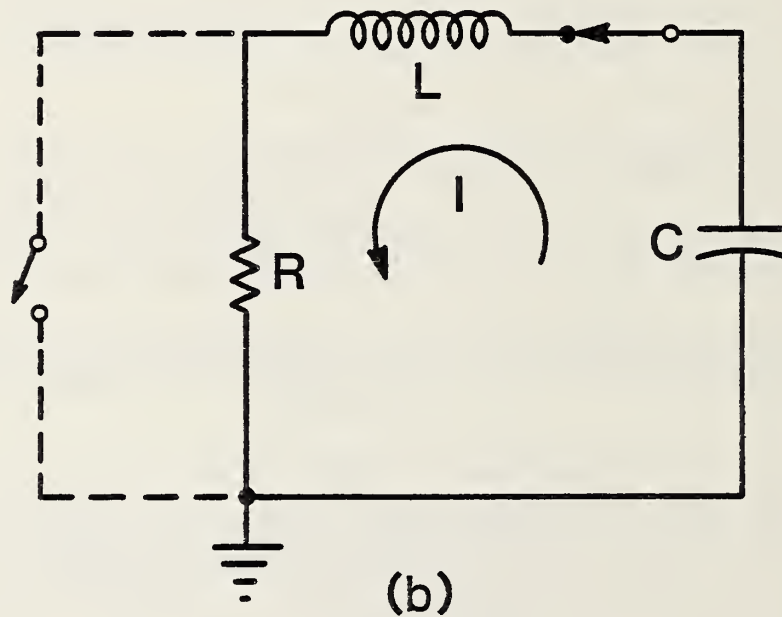
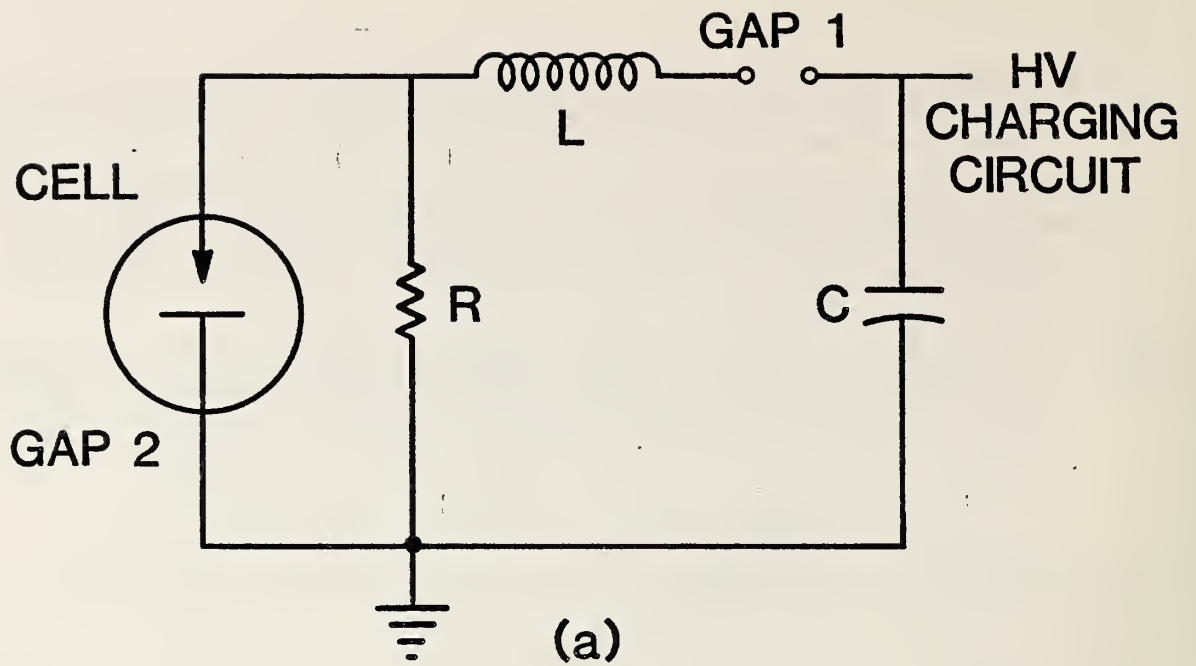


Figure 16. Pulse forming components to provide nanosecond rise time pulses:
 (a) actual circuit, (b) simplified pulse-shaping configuration, after the first gap has shorted, neglecting the cell.

further, the normalized voltage across the load, U, reduces to

$$U = e^{-(R/L)t} - e^{-t/RC}. \quad (22)$$

Within this approximation we see that L/R is the rise time constant of the pulse and RC is the fall time constant.

Returning to the exact expressions for the moment, another quantity of interest is the position of the peak of the applied pulse. Assuming the pulse starts at $t = 0$, the time the peak is reached is obtained by taking the derivative of eq (18) and setting it to zero. Solving for the time gives the time to reach the peak

$$T = [1/(a-b)] \ln(a/b). \quad (23)$$

The size of the pulse relative to the capacitor charging voltage is then obtained by evaluating eq (18) at time $t = T$. In table 3, we show a comparison of the types of pulse shapes which should be attainable based on these calculations.

Table 3. Pulse Shapes Based on RLC Component Values

R (Ω)	C (nF)	L (μ H)	$4L/(R^2)C$	TIME CONSTANTS		T (ns)	U PEAK
				RISE (ns)	FALL (ns)		
20	0.5	0.01	0.20	0.5	10	1.6	0.890
3.5k	2	1000	0.16	286	7000	972	0.904
10k	2	1000	0.02	100	20000	534	0.978
1k	1	100	0.4	100	1000	266	0.835
1k	1	1	0.004	1	1000	6.9	0.994
100	1	1	0.4	10	100	26.6	0.835

The first two lines of table 3 represent the anticipated extremes attainable in our laboratory. The results of these calculations indicate that it will be possible to attain sufficient regulation of the sub-microsecond pulse to allow exploration of nanosecond breakdown phenomena.

To test the feasibility of the above circuit design, a prototype was built to operate in air. Some measurements were performed on the air system, but because the stray inductances were small, the rise times as calculated above were faster than the measuring circuit. However, the fall times were as predicted from the above model. Additionally, it was shown that for the point-sphere electrode geometry used in gap 2 (see fig. 16a) it was easy to achieve breakdown within 200 ns of the time of application of the nanosecond rise time pulse.

Based on the results described above, the construction of a cell for studying liquid nanosecond breakdown was initiated this quarter. The electrode configuration which will first be tested will be the point-sphere geometry.

Small gaps will be required initially since the applied voltage will not exceed 100 kV. The circuit capacitor will be charged by either direct or pulsed voltage.

Next quarter will see the completion of the nanosecond breakdown cell and associated inductors to provide a wide selection of pulse shapes. Attempts will be made to photograph the temporal development of streamers using an image converter camera. The liquid used will be transformer oil. Some of our efforts will concentrate on the initial development of the streamer under high optical magnification.

For further information contact Dr. R. H. McKnight at (301) 921-3121.

6. REFERENCES

- [1] R. H. McKnight and P. M. Fulcomer, "Operation of Ion Counters near High Voltage DC Transmission Lines, to be published in proceedings, 4th International Symposium on High Voltage Engineering, Athens, 1983.
- [2] W. T. Kaune, M. F. Gillis, and R. J. Weigel, "Techniques for Estimating Space Charge Densities in Systems Containing Air Ions," J. App. Phys., 54, p. 6267, 1983.
- [3] NBS Report NBSIR 83-2761, Development of Power System Measurements--Quarterly Report, January 1 - March 31, 1983.
- [4] R. J. Van Brunt, T. C. Lazo, and W. E. Anderson, "Production Rates for Discharge Generated SOF_2 , SO_2F_2 , and SO_2 in SF_6 and $\text{SF}_6/\text{H}_2\text{O}$ Mixtures," Gaseous Dielectrics IV (L. G. Christophorou, ed.) Pergamon Press, New York (1984) pp. 276-285.
- [5] R. J. Van Brunt, "Production Rates for Oxyfluorides SOF_2 , SO_2F_2 , and SOF_4 in SF_6 Corona Discharges," NBS J. Res. (submitted, 1984).
- [6] "Development of Power System Measurements--Quarterly Report, January 1 1984 to March 31, 1984," R. Hebner, ed., Nat. Bur. Stand. (U.S.) NBSIR 84-2898 (1984).
- [7] R. J. Van Brunt and M. C. Siddagangappa, "Production Rates of Oxygenated Species in SF_6/O_2 and SF_6/N_2 Corona Discharges," Proc. 37th Gaseous Electronics Conf., Bull. Am. Phys. Soc. (to be published).
- [8] R. J. Van Brunt and W. E. Anderson, "Bibliography of Data on Electrical Breakdown in Gases," NBS Tech Note 1185 (1984).
- [9] K. Masek, L. Laska, V. Perina, and J. Krasa, "Some Peculiarities of the SF_6 and the $\text{SF}_6 + \text{O}_2$ Discharge Plasma," Acta. Phys. Slov., Vol. 33, pp. 145-150 (1983).
- [10] R. F. Hampson, "Chemical Kinetic and Photochemical Data Sheets for Atmospheric Reactions," U. S. Department of Transportation, Federal Aviation Administration Report No. FAA-EE-80-17 (1980).
- [11] A. C. Cristina and H. J. Schumacher, "The Kinetics and the Mechanism of the Thermal Reaction between Sulfurtetrafluoride and Fluorine," Z. Naturforsch., B: Anorg. Chem., Org. Chem., Vol. 36B, pp. 1381-1385 (1981).
- [12] "Development of Power System Measurements -- Quarterly Report, October 1, 1983 to December 31, 1983," R. Hebner, ed., Nat. Bur. Stand. (U.S.) NBSIR 84-2861 (1984).

U.S. DEPT. OF COMM. BIBLIOGRAPHIC DATA SHEET (See instructions)	1. PUBLICATION OR REPORT NO. NBSIR 85-3111	2. Performing Organ. Report No.	3. Publication Date February 1985
4. TITLE AND SUBTITLE Development of Power System Measurements -- Quarterly Report July 1, 1984 to September 30, 1984			
5. AUTHOR(S) R. E. Hebner, Editor			
6. PERFORMING ORGANIZATION (If joint or other than NBS, see instructions) NATIONAL BUREAU OF STANDARDS. DEPARTMENT OF COMMERCE WASHINGTON, D.C. 20234			7. Contract/Grant No. 8. Type of Report & Period Covered
9. SPONSORING ORGANIZATION NAME AND COMPLETE ADDRESS (Street, City, State, ZIP) Department of Energy Division of Electric Energy Systems 1000 Independence Avenue, SW Washington, DC 20585			
10. SUPPLEMENTARY NOTES <input type="checkbox"/> Document describes a computer program; SF-185, FIPS Software Summary, is attached.			
11. ABSTRACT (A 200-word or less factual summary of most significant information. If document includes a significant bibliography or literature survey, mention it here) <p style="text-align: center;">This report documents the progress on four technical investigations sponsored by the Department of Energy and performed by or under a grant from the Electrosystems Division, the National Bureau of Standards. The work described covers the period from July 1, 1984 to September 30, 1984. The report emphasizes the errors associated with measurements of electric and magnetic fields, the properties of corona in compressed SF₆ gas, the measurement of interfacial phenomena in transformer oil, and the measurement of dielectric properties on nanosecond time scales.</p>			
12. KEY WORDS (Six to twelve entries; alphabetical order; capitalize only proper names; and separate key words by semicolons) electric fields; gaseous insulation; interfaces; liquid insulation; magnetic fields; partial discharges; SF ₆ ; solid insulation; transformer oil			
13. AVAILABILITY <input checked="" type="checkbox"/> Unlimited <input type="checkbox"/> For Official Distribution. Do Not Release to NTIS <input type="checkbox"/> Order From Superintendent of Documents, U.S. Government Printing Office, Washington, D.C. 20402. <input checked="" type="checkbox"/> Order From National Technical Information Service (NTIS), Springfield, VA. 22161			14. NO. OF PRINTED PAGES 39 15. Price \$8.50

